

# Excitation of a Neuron for Characteristic Potential Generation

Yumi Takizawa and Atsushi Fukasawa  
 Institute of Statistical Mathematics, JAPAN  
 takizawa@ism.ac.jp

*Abstract:* - This paper presents unified modelling of excitation for generation of multiple output waveforms. Unified modelling is applied to neurons generating pulse and plateau with positive and negative potentials. Electro-physical analysis is given first that a  $p-n$  junction is formed in cytoplasm when positive charges are injected into cytoplasm filled with negative charges. The junction is characterized by a depletion layer between two zones. Modelling of a neuron is given by the configuration with three zones and two depletion layers induced in cytoplasm. Equivalent circuit and response are given for amplifier and generator (oscillator) of characteristic potentials of pulse and plateau, first for positive and then for negative potential excitations. Bipolar potential generation provides a neural system with accurate and reliable processing and transmission of information.

*Key-Words:* - Unified modelling of excitation, characteristic potential waveforms, pulse and plateau, positive and negative potentials,  $p-n$  junction, depletion layer, amplifier and generator.

## 1 Introduction

Potential pulse is generated in an excitatory cell, when reception potential exceeds threshold. Neuron and *paramecium* are regarded as excitatory cells. Positive and negative potentials are observed in *paramecium* for forward and backward movements by cilia[1].

Recently not only positive potential pulse and plateau but also negative potential plateau are observed in experiments of neurons[2,3].

A reasonable modelling of an active neuron has been proposed by the authors for positive potential pulse[4-6]. In this paper, it is shown that the above model is applied commonly to the models of generation of characteristic waveforms defined by polarities of potentials (positive and negative), and time durations (pulse and plateau).

At the beginning, it is needed to contrast the modelling of an active neuron by the authors with the earlier modelling.

Prior to the modelling by the authors[4-6], inferences and measurements were made under the condition essentially steady in time and uniform in space. The measurement of time was not involved, except in indication of action potential waveforms.

The practical measurements were made by the voltage (or current) clamp method, and a single electrode was inserted in cytoplasm.

Nevertheless, on the basis of these data, the earlier model was formed definitely by passive electrical circuit without feedforward gain and feedback ratio. (refer section 3.2, Fig.5, and Appendix A-2).

The model and analysis in this study are made respecting time- and space-dependent motions of  $\text{Na}^+$  and  $\text{K}^+$  in cytoplasm.

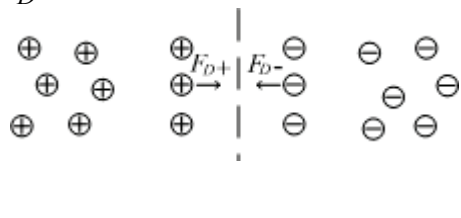
Electrical equivalent circuit is given for an operating neuron, which proves existence of feedback inside a neuron. Common basis of excitation in neurons will be presented on dual configuration with  $\text{Na}^+$  and  $\text{Cl}^-$  as the dominant charges (ions) for bipolar action potentials.

## 2 Characteristics of Liquid Junction in Cytoplasm

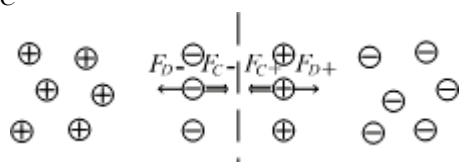
### 2.1 Formation of electrical zones and a depletion layer

When electric charges are injected into a zone in electrical medium, charge density at the zone becomes higher and the other zone remains lower. It is assumed that quantity of injected charges is little and velocity of charges is low in the medium. Special phenomena are induced at a boundary between two zones as shown in Fig. 1.

Phase 1: Diffusion of charges by gradient of density  $F_D$ .



Phase 2: Balance of diffusion  $F_D$  and Coulomb's force  $F_C$ .



Phase 3: Cease of diffusion and formation of,  
(a) p-zone and n-zone, and  
(b) space charges and depletion layer with depth  $d$ .

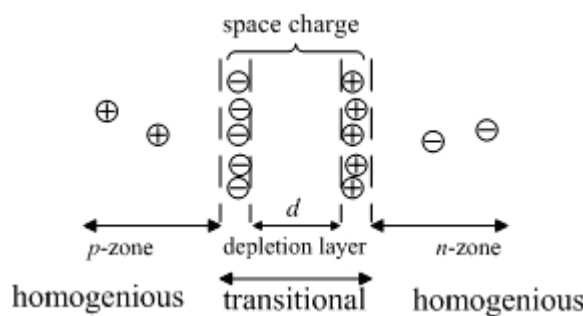


Fig. 1 Formation of zones and a depletion layer of a boundary.

Phase 1

Injected p-charges diffuse to n-zone, and n-charges diffuse to p-zone by the force of gradient of density  $F_D$ .

Phase 2

Coulomb's force  $FC$  (force by potential gradient) appears between diffused p- and n-ions. Directions of forces  $F_D$  and  $F_C$  are opposite. When they are balanced, diffusion is ceased.

Phase 3

A pair of space charges appears at both sides of the boundary. Potential difference appears in the boundary. And electric charges are driven outside the boundary, and two zones and a depletion layer (liquid junction) formed at the boundary.

## 2.2 Depth and capacity of depletion layer

Potential  $V(z)$  at a boundary is decided by true electric charge density  $\rho(z)$  based on the Poisson's equation.

$$\frac{d^2V(z)}{dz^2} = -\frac{\rho(z)}{\varepsilon_e} \quad (1)$$

where,  $z$  is the longitudinal axis of a neuron,  $\varepsilon_e$  is the permittivity of electrolyte solution.

True electric charge is defined as the charge unrestrained to any place. Then polarization charge at the membrane is removed from  $\rho(z)$ , because the polarization charge is restrained to the membrane in a neuron.

True electric charge density  $\rho(z)$  is given by the followings, and is shown as upper line in Fig.2.

$$\left. \begin{array}{l} \rho(z) = -q N_p \quad ; \quad -z_p \leq z \leq 0 \\ \rho(z) = +q N_n \quad ; \quad 0 \leq z \leq z_n \end{array} \right\} \quad (2)$$

where  $N_p, N_n$  are true electric charge densities at  $p$ - and  $n$ -side of the boundary.  $q$  is elementary electric charge.

The diffusion potential (liquid junction potential)  $V_D$  is defined as follows.

$$\begin{aligned} V_D &= V_n(z_n) - V_p(-z_p) \\ &= \frac{q}{2\varepsilon_e} (N_p z_p^2 + N_n z_n^2) \end{aligned} \quad (3)$$

$V_D$  is called as the height of potential wall for transmission of positive charge.

The depth of depletion layer is given as,

$$\begin{aligned} d &= z_p + z_n \\ &= \left( \frac{2\varepsilon_e (N_p + N_n)}{q N_p N_n} V_D \right)^{\frac{1}{2}} \end{aligned} \quad (4)$$

Now, bias voltage  $V_B$  is considered at the  $p$ -zone. Gradient of potential and charge density along positive ion channels causes equivalent voltage  $V_B$ . The polarity of  $V_D$  and  $V_B$  remains opposite.

$$d_B = \left( \frac{2\epsilon_e(N_p + N_n)}{qN_p N_n} (V_D + V_B) \right)^{\frac{1}{2}} \quad (5),$$

where,  $V_B$  corresponds to potential difference of ion channels injecting positive charges to  $p$ -zone in cytoplasm.

The positive charge  $Q$  per unit area at the boundary ( $n$ -side) is given as follows.

$$\begin{aligned} Q &= qN_n z_n = |-qN_p z_p| \\ &= \left( \frac{2\epsilon_e q N_p N_n}{N_p + N_n} (V_D + V_B) \right)^{\frac{1}{2}} \end{aligned} \quad (6)$$

The structure is assumed as an equivalent capacity.

$$c = \left| \frac{dQ}{dV} \right| = \left( \frac{\epsilon_e}{2} \frac{q N_p N_n}{N_p + N_n} \frac{1}{V_D + V_B} \right)^{\frac{1}{2}} \quad (7)$$

When  $V_B$  is applied forwardly at the boundary, the height of the potential wall becomes lower.

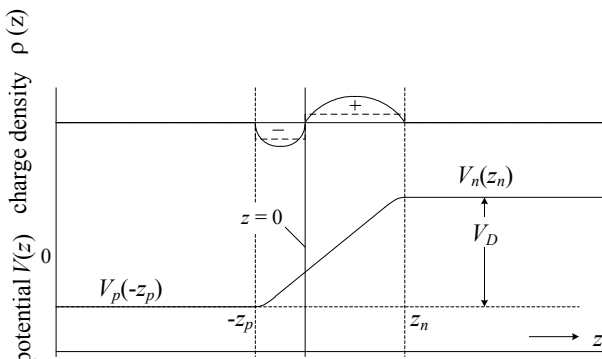


Fig. 2 Distribution of true electric charge and diffusion potential of a boundary.

Upper: Distribution of true electric charge density  $\rho(z)$ . Dotted line shows approximation for calculation.

Lower: Potentials  $V_p$ ,  $V_n$ , and diffusion potential  $V_D$ .

### 3 Excitation of a Neuron for Positive Potential Generation

#### 3.1 Electro-physical modelling for positive potential generation

##### 3.1.1 Electrical zones and depletion layers

Electro-physical modelling is given in Fig. 3. Three zones are assigned for the dendrite (input), the central part (ground), and the axon (output). The potential at each zone is specified by electrical charges of  $p$ - and  $n$ -ions. The first and the second depletion layers are assigned between zones.

This formation is dependent to the time and motion of charges at zones and depletion layers. Interaction of parameters (charge, potential, energy) along zones and depletion layers are analysed as follows.

##### 3.1.2 Ion channels

$\text{Na}^+$  channels for reception of neurotransmitter from previous neurons are ligand dependent.  $\text{Na}^+$ ,  $\text{K}^+$ , and  $\text{Cl}^-$  channels at the central part and at the axon are voltage dependent.  $\text{Ca}^{2+}$  channels are provided for secretion of neurotransmitters.

$\text{Na}^+$ - $\text{K}^+$  transporter (ion pump) operates to provide resting potential which works as a battery for neural circuit.

##### 3.1.3 Electrical parameters

Positive input charges at the dendrite are partially lost by recombination with existing negative charges, and most of charges arrive at the axon. However positive potential is amplified by output and input impedance ratio.

As the result, voltage gain  $G \gg 1$ , current multiplication factor  $\alpha \approx 1$  in Chapter 2 and 3.

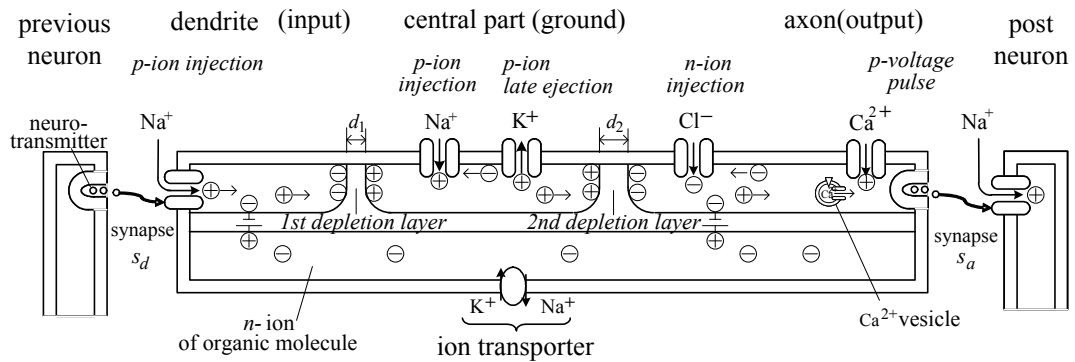


Fig. 3 Electro-physical modelling for positive potential waveform generation.  
All branches of dendrite and axon are collected to single port respectively.  
 $Na^+$  channels at the dendrite is ligand-dependent. Ion channels at the central part and at the axon are voltage-dependent.  $Na^+$  channels are not at the axon. Late ejection of  $K^+$  causes for active potential to return rapidly to resting.  $Ca^{2+}$  channels and  $Ca^{2+}$  vesicles are for secretion of neurotransmitter.  $Na^+ - K^+$  transporter works as a battery. Injection of  $Cl^-$  and ejection of  $K^+$  at the axon provide same effect electro-physically.

### 3.2 Formulation of excitation for positive potential

#### 3.2.1 Electrical modelling of excitation

Electrical modelling of excitation for positive potential waveform is shown in Fig.4. Input and output diodes  $n_d$ ,  $n_a$  correspond to the first and the second depletion layers in Fig.3.

$\alpha$  is current multiplication factor,  $\alpha \cdot i_d$  is equivalent current source for output circuit.  $r_c$  is resistance giving feedback from output to input.

Configuration of excitation with forward and reverse diodes in Fig.4 corresponds to energy diagram of charges shown in Fig. A-1.

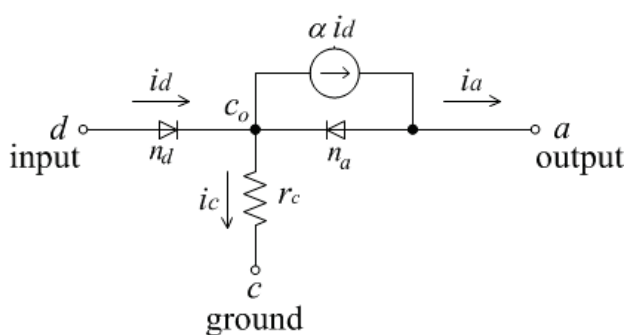


Fig. 4 Electrical modelling of excitation of a neuron for positive potential waveform generation.

#### 3.2.2 Characteristics as an amplifier

Electrical modelling of an active neuron is shown in Fig. 5. The points of  $d_0$ ,  $a_0$  are the outside points of membrane.  $c_0$  is a virtual point taken in the central part.

Impedances  $r_d$  and  $r_a$  of forward and reverse diodes,  $n_d$  and  $n_a$  are low and high resistances respectively.  $r_d$  and  $r_a$  depend on potential heights at the first and the second depletion layers.

Impedance ratio  $r_a / r_d$  is kept large enough to limit coupling of output to input circuits.

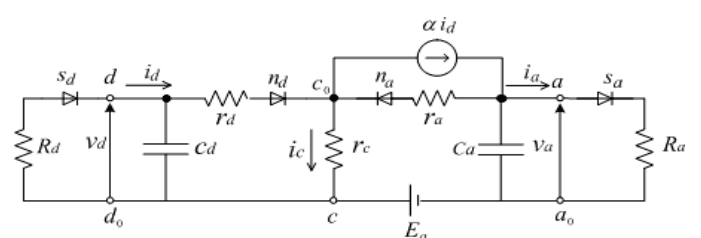


Fig. 5 Electrical modelling for positive potential waveform generation.

The capacitances  $C_d$  and  $C_a$  are caused by the first and the second depletion layers. Input and output synapses  $s_d$  and  $s_a$  are shown as forward diodes for excitatory synapses ( $p$ -ions). Potential  $E_a$  is derived with ion transporter (ion pump) in Fig. 3.

It is estimated that  $G_i$  current gain (current multiplication factor) is 1 approximately. So energy gain is equivalent to voltage gain. Where, voltage gain  $G_v$  is given by ratio of output impedance (high) and input impedance (low).

Voltage amplification gain  $G_v$  is given as;

$$G_v = \frac{v_a}{v_d} = \frac{\frac{\alpha R_a}{r_d + r_c}}{1 - \frac{\alpha R_a}{r_d + r_c} \cdot \frac{r_c}{R_a}} = \frac{K}{1 - K\beta} \quad (8)$$

$$K = \alpha \frac{R_a}{r_d + r_c} \quad (9)$$

$$\beta = \frac{r_c}{R_a} \quad (10)$$

where,  $v_d$  and  $v_a$  are input and output voltages of a neuron,  $G_v$ ,  $K$ ,  $\beta$  are closed loop gain, open loop gain, and inner feedback ratio of a neuron respectively. Oscillation condition is given by  $K\beta \geq 1$ . (ref. Appendix A-3)

In case that the axon has little Cl channels,  $\alpha < 1$ ,  $K\beta \ll 1$ . Therefore a neuron operates as an amplifier with threshold for input signal with positive inner feedback.

### 3.2.3 Characteristics as a generator of positive potential waveforms

The neuron operates as a generator of positive potential output when the product of open loop gain  $K$  and feedback ratio  $\beta$  exceeds 1.

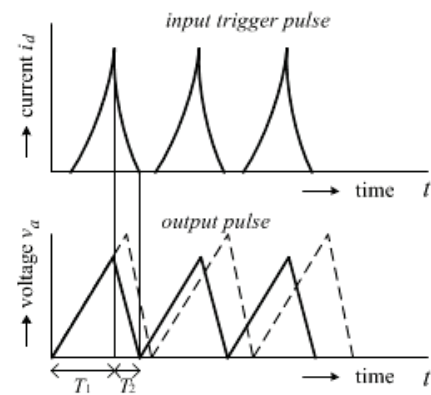


Fig.6 Output voltage waveform for positive potential waveform generation. The dotted line is an original waveform. The solid line is synchronized waveform to the input trigger pulse.

This generator is composed of self-injection with inner feedback signal without external trigger.

$$T_1 = C_d \frac{r_c R_a}{r_c + R_a} \quad (11)$$

$$T_2 = C_a R_a \quad (12),$$

where,  $R_d + r_d \gg r_c$ ,  $r_a = \infty$

are assumed for simplified analysis.

The pulse time width  $T$  is given as the total time length as following;

$$T = T_1 + T_2 = C_d \frac{r_c R_a}{r_c + R_a} + C_a R_a \quad (13).$$

The mode of oscillation is astable. Here, “Astable” means not unstable but the mode without stable point except 0 in amplitude.

The neuron operates tuned to external injection. Whenever, the phase and the period of original free running oscillator is fluctuating, the oscillator becomes stable by locking to the external signal as shown in Fig. 6.

Synchronization is established in a system with group of neurons, and stable timing clock is realized by whole coupling among neurons (Appendix A-3).

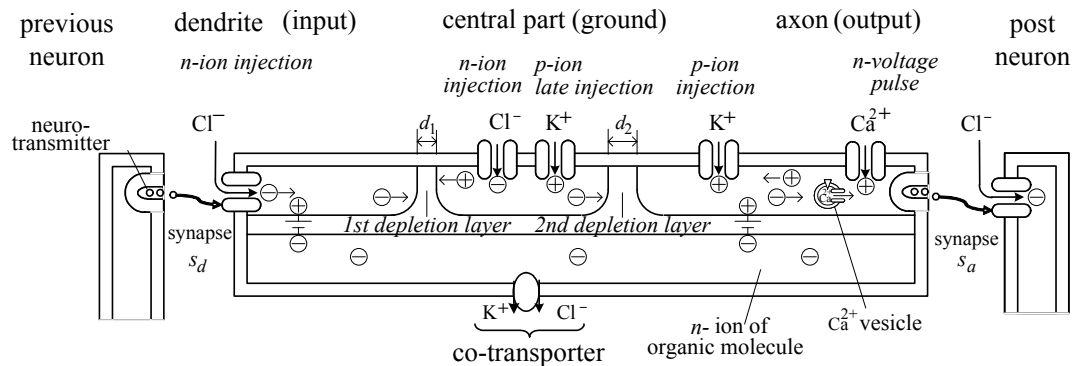


Fig. 7 Electro-physical modelling of an active neuron for negative potential waveform generation.  $\text{Cl}^-$  channels at the dendrite is ligand-dependent. Ion channels at the central part and at the axon are voltage-dependent. Injections of  $\text{K}^+$  and  $\text{Na}^+$  at the axon give same effect electro-physically.

## 4 Excitation of a Neuron for Negative Potential Generation

### 4.1 Electro-physical modelling for negative potential generation

Electro-physical modelling of a neuron for negative waveform is given in Fig. 7.

Formation of zones and depletion layers in Fig. 7 is same to Fig. 3 except the kinds of ion channels. Ion channels for reception of signals from previous neurons are ligand-dependent  $\text{Cl}^-$  channels

Ion channels for reception of signals from previous neurons are ligand dependent  $\text{Cl}^-$  channels.  $\text{Cl}^-$  and  $\text{K}^+$  channels at the central part and at the axon are voltage dependent.  $\text{Ca}^{2+}$  channels are provided for secretion of neurotransmitters.

$\text{K}^+$   $\text{Cl}^-$  co-transmitter operates to provide resting potential which works as a battery for neural circuit [7].

### 4.2 Formulation of excitation for negative potential

Electrical modelling of excitation for negative waveform is shown in Fig. 8. Input and output diodes  $n_d$ ,  $n_a$  correspond to the first and the second depletion layers, which are shown as reverse and forward diodes respectively.

Equivalent circuit of active neuron is shown in Fig. 9 for negative potential waveform generation.

For negative potential waveform generation, the waveform is just inverse of the waveform shown in Fig. 10.

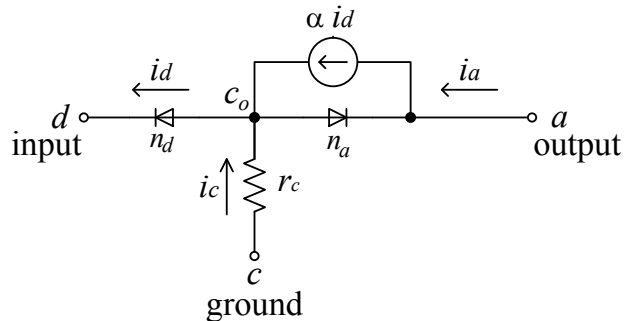


Fig. 8 Electrical modelling of excitation of a neuron for negative potential waveform generation.

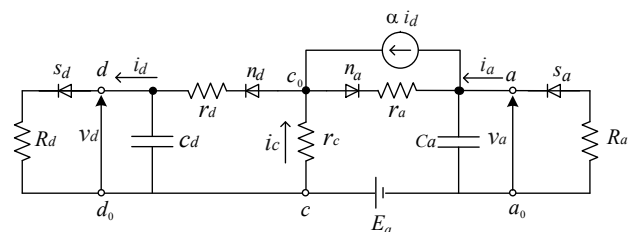


Fig. 9 Electrical modelling of an excitatory cell of neuron for negative potential waveform generation.

## 5 Characteristic Potential Waveforms

Varieties of characteristic potential waveforms have been observed in experiments of neurons and unicellular organism. Significant difference exists in time duration of waveforms (spike and plateau). Variation of waveform is performed by modulation with ion channels prepared at the dendrite (input) and at the central part (control).

### 5.1 Pulse (spike)

Ligand-dependent  $\text{Na}^+$  channels are first considered at the dendrite (input) in Fig. 1.

$\text{Na}^+$  channels open quickly after reception of neurotransmitter. By late ejection (efflux) of  $\text{K}^+$ , the potential at the central part (control) return rapidly from active (positive) to resting (negative) potentials. Ejection of  $\text{K}^+$  are executed fast by the same directions of driving forces of diffusion  $F_d$  and Coulomb potential  $F_C$ , [6]. Then the return time  $T_2$  in Fig. 4 for positive potential waveform becomes sufficiently short pulse at the axon (output).

Ligand-dependent  $\text{Cl}^-$  channels are also considered at the dendrite (input) in Fig. 5.

$\text{Cl}^-$  channels open quickly after reception of neurotransmitter. By late injection (influx) of  $\text{K}^+$ , the potential at the central part (control) returns quickly from active (deeply negative) to resting (negative) potentials. Injection of  $\text{K}^+$  are done a little late by the opposite directions of  $F_d$  and  $F_C$ . Then the return time  $T_2$  of negative potential waveform takes a little longer compared to positive potential waveform.

### 5.2 Plateau

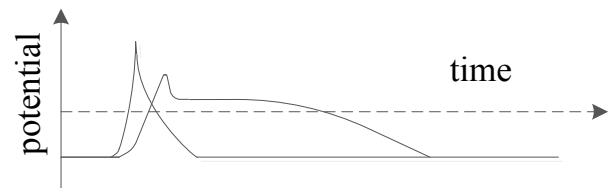
Metabotropic  $\text{Na}^+$  channels are secondly considered at the dendrite (input) in Fig. 1.

$\text{Na}^+$  channels open lately after reception of the first messenger by chemical process for the second messenger in cytoplasm.

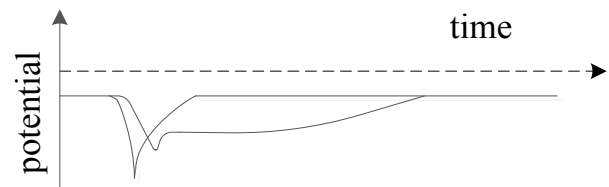
Voltage dependent  $\text{Na}^+$  channels at the central part and at the axon produce plateau to hold time for steady operation.

Metabotropic  $\text{Cl}^-$  channels are also considered at the dendrite (input) in Fig. 5.

$\text{Cl}^-$  channels open lately after reception of the first messenger by chemical process for the second messenger in cytoplasm.



(a) Positive potential waveform



(b) Negative potential waveform

Fig. 10 Characteristic potential waveforms of pulse and plateau with positive and negative potentials.

Voltage dependent  $\text{Cl}^-$  channels at the central part and at the axon produce plateau output potential to provide holding time for steady operation.

### 5.3 Modelling of output potential waveforms

Modellings of typical output potential waveforms for excitatory neurons are given in Fig. 10 based on the above schemes of excitation. Output waveforms are drawn by superimposing.

## 6 Conclusion

Until today, function of excitation of a neuron has been interpreted as capability of positive potential (pulse and plateau) generation. Negative potential generation has been interpreted as operation of suppression (inhibition) of positive potential generation.

Based on electro-physical and electrophysiological basis of excitatory cells, this paper shows that not only positive potential but also negative potential is generated and utilized in neural systems. Negative potential generation has already been observed in the experiment in neural systems of aplysia [2,3] and in a cell of *paramecium* and *noctiluca* of unicellular animals.

## References:

- [1] Naitoh Y., Eckert R., Ionic mechanisms controlling behavioral responses of paramecium to mechanical stimulation, *Science*, 164, pp. 963-965, 1969.
- [2] MacCaman R. E., Weinreich D., On the nature of histamine mediated slow hyperpolarizing synaptic potentials in identified molluscan neurons, *Journal of Physiol.*, 328, pp. 485-506, 1982.
- [3] Sasaki K., et al, A single GTP-binding protein regulates K<sup>+</sup>-channels couples with dopamine, histamine and acetylcholine receptors, *Nature*, Fig. 1, 325, 259, 1987.
- [4] Fukasawa A., Takizawa Y., Activity of a Neuron and Formulation of a Neural Group for Synchronization and Signal Processing, *Proc. of the Int. Conf. on Neurology*, pp.242-247, Kos, Greece, July 2012, "The Best Paper Prize of NEUROLOGY'12" awarded by WSEAS/NAUN.
- [5] Fukasawa A., Takizawa Y., Activity of a Neuron and Formulation of a Neural Group for Synchronized Systems, *International Journal of Biology and Biomedical Engineering*, Issue 2, vol. 6, pp. 149-156, 2012.
- [6] Fukasawa A., Takizawa Y., Activity of a Neuron and Formulation of a Neural Group based on Mutual Injection in keeping with system synchronization, *Proc. of International conference on Circuit, Systems, Control, Signals (CSCS'12)*, pp. 53-58, Barcelona, Spain, Oct. 17, 2012.
- [7] Okada Y., Ion channels and Transporters Involved in Cell Volume Regulation and Sensor mechanisms, *Cell Biochemistry and Biophysics*, vol.41, pp.233-257, 2004.
- [8] Kamada T., Some observations on potential difference across the ectoplasm membrane of Paramecium, *Journal of Experimental Biology*, vol. 11, pp.94-102, 1934.
- [9] Takizawa Y., Fukasawa A., Formulation of Topographical Mapping in Brain with a Synchronous Neural System, *Proceedings of the 15th International Conference on Mathematical Methods, Computational Techniques and Intelligent Systems (MAMECTIS'13)*, pp. 60–65, Lemesos, Cyprus, Mar. 21-23, 2013.
- [10] Takizawa Y., Fukasawa A., Formulation of a Neural System and Analysis of Topographical Mapping in Brain, *International Journal of Biology and Biomedical Engineering*, Issue 2, vol. 6, pp. 157-164, 2012.
- [11] Takizawa Y., Fukasawa A., Electrical Measurement Scheme of Liquid Boundaries in Active Neuron, *Proc. of Int. Conf. on Health Science and Biomedical Systems (HSBS'14)*, pp. 11-15, Nov. 22, 2014.
- [12] Takizawa Y., Fukasawa A., Topographical Mapping by a Synchronous Neural System with Physical Measures of Time, Space, and Motion, *International Journal of Biology and Biomedical Engineering*, vol. 8, pp.63-69, 2014.
- [13] Catsigeras E., Self-synchronization of networks with a strong kernel of integrate and fire excitatory neurons, *WSEAS Transactions on Mathematics*, Issue 7, vol. 12, Section 5, p. 794, July 2013.
- [14] Shockley W., *Electrons and holes in semiconductors*, Fig. 4, pp. 112-113, D. Van Nostrand, New York, 1950.
- [15] Takizawa Y., Rose G., Kawasaki M., Resolving Competing Theories for Control of the Jamming Avoidance Response: The Role of Amplitude Modulations in Electric Organ Discharge Decelerations, *Journal of Exp. Biol.* 202, pp. 1377-1386, 1999.
- [16] Fukasawa A., Takizawa Y., Activities of Excitatory Cells of Neuron and Unicellular Organism, *International Journal of Biology and Biomedical Engineering*, vol. 9, pp. 98-103, 2015.
- [17] Fukasawa A., Takizawa Y., Activity of a Neuron for Generation of Pulse and Plateau with Positive and Negative Potentials, *Proc. of Health Science and Biomedical Systems (HSBS'15)*, pp.65-71, Aug., 2015.
- [18] Takizawa Y., Fukasawa A., Takeuchi H. A., Positive and Negative Action Potentials in *Paramecium* relating to Neurons, *Proc. of Health Science and Biomedical Systems (HSBS'15)*, pp.54-60, Aug., 2015.

## Appendix

### A.1 Energy Diagram of Electrical Charges

Energy diagram for Fig.3 and 7 is shown commonly in Fig. A1 [4-6].

Energy difference of *p*- and *n*-ions is small. Solid line is given as the Fermi level for mean energy of *p*- and *n*-ions.

The energy at the dendrite becomes high by signal *p*-ion injection. The energy at the central part then becomes high, but lower than the previous. Signal *p*-ions pass over the first potential wall easily.

At arrival of signal *p*-ions at the second depletion layer with higher potential wall, signal *p*-ions pass over by the thermal motion. High energy is given to *p*-ions at the axon.

$\text{Cl}^-$  ions enhance the energy at the axon as the solid line over the dotted line for the axon without  $\text{Cl}^-$  ion channel. The effect of  $\text{Cl}^-$  ions fed at the axon terminal is just equal to the effect of electrons fed at the collector end.

The first and the second depletion layers in Fig. A1 correspond to forward and backward diodes in Fig. 4 and 8.

The equivalent circuit composed by forward and reverse diodes corresponds to signs of gradient of energy at the first and the second depletion layers.

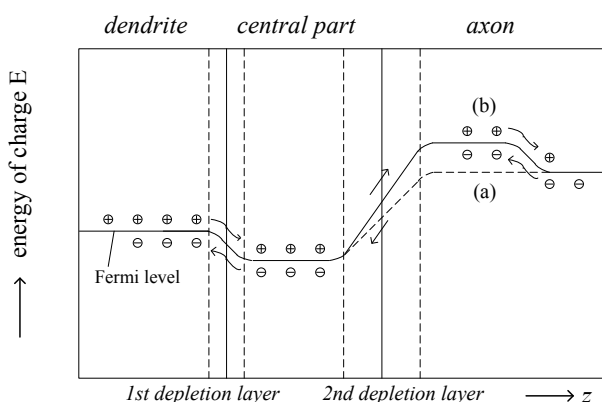


Fig. A1 Energy diagram of positive and negative ions. *z*-axis (horizontal) denotes point along signal transmission direction. Solid and dotted lines show energy at the axon (a) without and (b) with  $\text{Cl}^-$  channels. The effect of (b) is removed from the analysis in equation in Chapter 3 and 4.

### A.2 Transfer functions for feedback and feedforward loops

#### (a) Transfer function of feedback loop

Transfer function is given by feedback loop with feedforward gain *K* and backward ratio  $\beta$  as shown in Fig. A2.

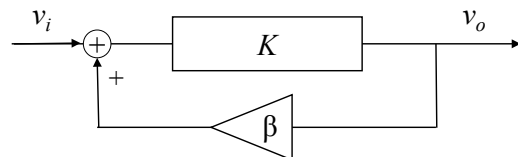


Fig. A2 Positive feedback (regenerative) system.

The output is given by the following equation.

$$v_o = K(v_i + \beta v_o), \quad (\text{A-1}),$$

$$\frac{v_o}{v_i} = \frac{K}{1 - K\beta} \quad (\text{A-2}).$$

In the case of the negative feedback system, frequency characteristics is improved wider. Oscillation (excitation) condition is defined by forward gain and feedback ratio.

#### (b) Transfer function of feedforward system

Transfer function is given by summation of feedforward gain *K* and ratio  $\alpha$  (Fig. A3). This is different to regeneration.

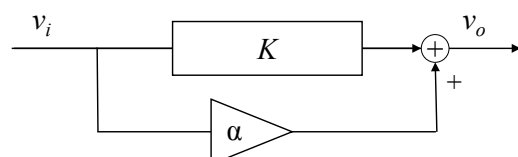


Fig. A-3 Positive feedforward system.

The output is given by the following equation.

$$v_o = K v_i + \alpha v_i, \quad (\text{A-3}).$$

$$\frac{v_o}{v_i} = K + \alpha \quad (\text{A-4}).$$

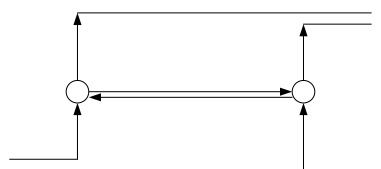
This function is only amplification. Oscillation is impossible by feedforward transfer function.

### A.3 Self-Systematization by Mutual Pulse Injection among Neurons

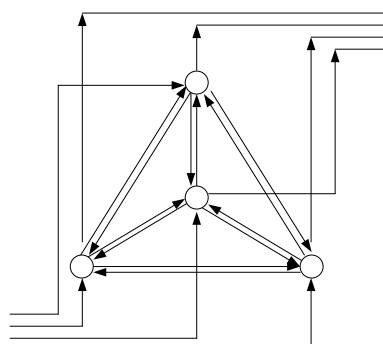
Actual formation of a neural group is given in Fig. A4. A small circle represents a neuron. Input and output signals of a neuron are at a branch of the dendrite and at a branch of the axon. A set of pair neurons is shown in Fig. A4 (a). Connection between two neurons is performed by arrows with dual directions. A system of four neurons is shown in Fig. A4 (b).

The timing of output pulse of an oscillator is adjusted by the other. When two oscillators are connected with each other, the timing is set at a certain timing between two. As number of oscillators increases, the variation of timings among neurons is reduced and system synchronization is established.

This formation enables system synchronization and synchronized signal processing simultaneously. Signal processing for multiple inputs and multiple outputs are available for dynamic processing including correlation, comparison, and detecting variations. This formation will be required for complex, reliable, and fast operation and signal processing [5,6,9-13]



(a) A set of two neurons.



(b) A system by four neurons.

Fig. A4 Synchronization and signal processing by mutual injection.